# Modified transfer matrix for nanostructures with arbitrary potential profile

S. A. Rakityansky*
*Department of Physics, University of South Africa, P.O. Box 392, Pretoria 0003, South Africa*
(Received 6 April 2004; revised manuscript received 7 September 2004; published 17 November 2004)

A method is developed for solving the problems of bound, scattering, and resonant states of charge carriers in semiconductor nanostructures within the effective-mass envelope-function approach. On each interval of the effective-mass constancy, the Schrödinger equation is replaced by an equivalent system of linear first-order differential equations whose solutions are used to construct the modified transfer matrix by matching them via the Ben-Daniel–Duke–Bastard procedure at the points of the effective mass discontinuity. In contrast to the traditional transfer matrix theory where the potential energy is approximated by a sequence of rectangular steps, the proposed method is able to deal with an arbitrary potential profile directly and in an exact way, i.e., without resorting to the plane-wave approximation at each step. Therefore, the number of factors in the total transfer matrix is always equal to the number of intervals where the effective mass remains constant, no matter how complicated the potential profile. After the transfer matrix is obtained, the Jost matrix that totally determines the interaction properties, can be easily constructed. Zeros of its determinant in the complex energy plane correspond to bound states and resonances. Within the proposed method there is a natural way of inclusion of the long-range potential tails that may arise, for example, due to the charge accumulation. The pure Coulomb tails are taken into account in an exact way, i.e., analytically. An additional feature of the proposed method is the possibility of calculating not only the total widths of resonances but their partial widths as well. The effectiveness and accuracy of the method are demonstrated by several numerical examples.

DOI: 10.1103/PhysRevB.70.205323 PACS number(s): 73.63.−b, 73.23.−b

## I. INTRODUCTION

The artificially grown crystals, known as one-dimensional superlattices, nanostructures, nanodevices, mesoscopic devices, and semiconductor heterostructures, are composed of alternating layers of different semiconductor materials with nanometer thickness (see, for example, Ref. 1). For the electrons and holes moving perpendicularly to the layers, they represent a one-dimensional alternating sequence of potential wells and barriers. In principle, the properties of nanodevices can be changed at will by adjusting the chemical composition and thickness of the layers, i.e., by constructing a given potential profile, to suit specific applications.

Thanks to advances in epitaxial growth technology, it has become possible to make nanodevices with practically any given potential profile. The problem is how to choose an optimal profile that would generate the desired spectrum of bound states and resonances as well as the desired charge distribution (wave function profile) inside the structure. This requires reliable methods for theoretical analysis of the motion of charge carriers through the structure.

Several methods for locating the bound states and resonances generated by one-dimensional potentials have been developed over the past decades (for references and review of the existing methods, see Ref. 2). Practically all of them are based on the so-called transfer-matrix approach. In essence, this approach consists in the discretization of the potential profile by a sequence of thin elements of rectangular shape with constant potential energy. For each of these elements, the wave function is a superposition of the right and left traveling plane waves. The superposition coefficients in two adjacent elements are related via the so-called transfer matrix constructed to satisfy the continuity condition. Then the total transfer-matrix for the whole physical structure is a product of the elementary matrices.

The spectral points, i.e., bound states and resonances, are those points in the complex energy plane, at which the wave function has only outgoing waves outside the structure. These points, therefore, are sought by requesting that the total transfer matrix transforms an outgoing wave at the right end into an outgoing wave at the left end of the structure.

This relatively simple transfer-matrix approach is rather universal although it is not suitable in some cases. For example, it is difficult to use the standard transfer matrix when the potential has slowly decaying tails outside the physical structure (for instance, when charge is accumulated on the surfaces). The rectangular discretization is also not satisfactory when the potential profile has segments of fast variations (near impurities, for instance) or is biased by strong electric field[3] (Stark effect). There is a modification of the method that uses the trapezoidal discretization instead of the rectangular one.[4] The trapezoidal segments can approximate the potential more accurately. However, to achieve high accuracy, one still has to subdivide the interval in too many elements when the potential is not simple.

In Ref. 5 an exact and unified method was developed for finding a complete solution of the one-dimensional Schrödinger equation at any complex energy and for an arbitrary potential profile. Based on a system of linear first-order differential equations that are equivalent to the Schrödinger equation, this method is very efficient and accurate in locating not only bound states and narrow resonances but extremely wide and overlapping resonances as well. It is also able to adequately take into account long-range tails of the potential. The only drawback of the method of Ref. 5 is that it was designed for a system with constant effective mass. In the real-life problems, however, the effective mass of the charge carriers (electrons or holes) is different inside semiconductor layers with different chemical compositions.

 

In the present paper, the method is further developed to accommodate it to such problems.

To this end we employ the idea of the transfer matrix method but in a different way. The modification proposed in the present work, enables us to get rid of the rectangular discretization altogether. This is achieved by using general solution (i.e., two linearly independent solutions) of the Schrödinger equation on each interval of the effective mass constancy. Then the physical wave function is constructed as a linear combination of these basic solutions (instead of the plane waves) and the combination coefficients on the adjacent intervals are related by a $2\times 2$ matrix which may be called the modified transfer matrix. The number of the elementary factors in such modified transfer matrix for the whole system is always equal to the number of intervals of the effective-mass constancy, no matter how complicated the potential is on these intervals.

Another advantage of the proposed method is the possibility not only to locate the spectral points but to obtain in one run a complete solution of the problem, including the Jost matrix, *S*-matrix, and the wave function. Moreover, knowledge of the Jost matrix enables us to calculate the partial widths of a resonance, that determine relative probabilities of its decay into the left and right channels.

The effectiveness and accuracy of the suggested approach are demonstrated by several numerical examples where the motion of particles through biased quantum-well semiconductor heterostructures as well as in a potential with infinite tails is considered.

## II. STANDARD TRANSFER MATRIX

The standard transfer-matrix method consists of the following steps. First of all, one starts from the envelope-function approximation, which means that the motion of a charged particle through a nanostructure is described by the effective-mass Schrödinger equation

$$\left[-\frac{\hbar^2}{2}\frac{d}{dz}\frac{1}{\mu(z)}\frac{d}{dz}+\mathsf{V}(z)-E\right]\psi(E,z)=0, \tag{1}$$

where the effective mass $\mu$ changes with the coordinate $z$. In practice, it is assumed that $\mu(z)$ is a sectionally constant function. For example, in the structure formed by the sequence of GaAs and $Al_xGa_{1-x}As$ layers, the effective mass of the electron is determined by the aluminum mole fraction $x$, namely, $\mu=0.067\ m_e$ inside the GaAs layers and $\mu=(0.067+0.083x)m_e$ in the layers containing aluminum ($m_e$ is the free-electron mass). Therefore, for each layer, Eq. (1) becomes an ordinary Schrödinger equation with a constant mass. But the mass is different for different layers.

The second important step in the traditional transfer-matrix approach is the rectangular discretization. The potential profile is replaced by a sequence of thin elements of rectangular shape with constant potential energy. In the simplest case, when the system is not biased by an external electric field and when the space charge is not accumulated anywhere, these rectangular elements coincide with the physical layers. If, however, the potential profile is more complicated (which is the case practically always), it is approximated by a ladder of rectangular steps (see an example in Fig. 1). For each of these rectangular elements, Eq. (1) looks very simple

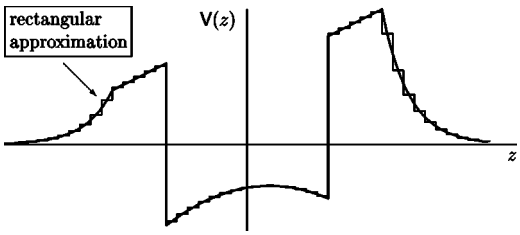


FIG. 1. An example of using the rectangular steps (ladder approximation) in order to adapt a one-dimensional potential for traditional transfer matrix method.

$$\frac{d^2}{dz^2}\psi_n(E,z)+k_n^2\psi_n(E,z)=0, \tag{2}$$

where the momentum

$$k_n^2=\frac{2\mu_n}{\hbar^2}(E-\mathsf{V}_n), \tag{3}$$

is determined by the constant values $\mathsf{V}_n$ of the potential and the effective mass $\mu_n$ in the $n$th element. Two linearly independent solutions (the fundamental system of solutions) of Eq. (2) are the right and left traveling plane waves and, therefore, the physical wave function is a superposition of them

$$\psi_n(E,z)=A_n^{(+)}(E)e^{ik_nz}+A_n^{(-)}(E)e^{-ik_nz}. \tag{4}$$

On the border between two adjacent elements the wave function is continuous,

$$\psi_n(E,z_n)=\psi_{n+1}(E,z_n), \tag{5}$$

and its derivative obeys the so-called Ben-Daniel—Duke—Bastard matching condition

$$\frac{1}{\mu_n}\psi_n'(E,z_n)=\frac{1}{\mu_{n+1}}\psi_{n+1}'(E,z_n). \tag{6}$$

By matching the wave function in two adjacent elements through these two conditions, it is easy to show (see, for example, Ref. 1) that the plane-wave amplitudes of Eq. (4) are related via a $2\times 2$ matrix which is called the transfer matrix,

$$\begin{pmatrix}A_n^{(+)}(E)\\A_n^{(-)}(E)\end{pmatrix}=\mathcal{Q}_{n,n+1}(E)\begin{pmatrix}A_{n+1}^{(+)}(E)\\A_{n+1}^{(-)}(E)\end{pmatrix}.$$

Then the total transfer-matrix for the whole physical structure (approximated by $N$ rectangular elements) is a product of the elementary matrices,

$$\begin{pmatrix}A_0^{(+)}\\A_0^{(-)}\end{pmatrix}=\mathcal{Q}_{0,1}\mathcal{Q}_{1,2}\mathcal{Q}_{2,3}\ldots\mathcal{Q}_{N,N+1}\begin{pmatrix}A_{N+1}^{(+)}\\A_{N+1}^{(-)}\end{pmatrix}.$$

This product is also a $2\times 2$ matrix

$$\mathcal{Q}_{0,1}\mathcal{Q}_{1,2}\mathcal{Q}_{2,3}\cdots\mathcal{Q}_{N,N+1} \equiv \begin{pmatrix} q_{11}(E) & q_{12}(E) \\ q_{21}(E) & q_{22}(E) \end{pmatrix}$$

that relates the superposition coefficients $A_n^{(\pm)}$ of the two elements with numbers $n=0$ and $n=N+1$, situated at the left and right ends of the $z$ line (outside the physical structure).

The spectral points, i.e., bound states and resonances are those points of the complex energy surface, at which the wave function has only outgoing waves in the outside regions of the line. From this point of view, the only difference between the bound and resonant states is that the former are on the negative real axis while the latter in the fourth quadrant of the unphysical sheet of the Riemann $E$ surface (see Ref. 5).

As one can easily see, the matching procedure involves the momentum $k_n$ and, therefore, all the matrix elements of $\mathcal{Q}_{n,n+1}$ depend on the energy $E$. The bound states and resonances are zeros of $q_{11}(E)$ in the complex energy plane. Indeed, a solution with outgoing waves at both ends of the line,

$$\begin{pmatrix} 0 \\ A_0^{(-)} \end{pmatrix} = \begin{pmatrix} q_{11}(E) & q_{12}(E) \\ q_{21}(E) & q_{22}(E) \end{pmatrix} \begin{pmatrix} A_{N+1}^{(+)} \\ 0 \end{pmatrix},$$

is only possible if

$$q_{11}(E) = 0.$$

The zeros of this equation found on the real negative axis correspond to bound states and those in the fourth quadrant, to resonances. The above scheme is described, for example, in Ref. 6 where its efficiency is proved by comparison with several other methods of solving one-dimensional Schrödinger equation.

In principle, any reasonable smooth curve can be approximated by a ladder of short horizontal steps, and therefore, it seems that the traditional transfer-matrix approach with its rectangular discretization is able to treat any potential profile. This, however, is only partially true. In practice, when the accumulated charge and impurities are taken into account, one deals with rapidly varying potentials that can also have long-range tails outside the physical structure. As a result, in many cases one has to use either too short ladder steps or too many of them in order to achieve reasonable accuracy. On the other hand, too large number of steps may cause numerical instabilities. In order to fight them, one has to devise special methods such as the recurrence technique of Ref. 7.

Furthermore, when taking into account the space charge of the current, one has to solve a self-consistent problem by iterations.[8] At each new iteration, the potential profile is changing and a new discretization pattern might be needed. Moreover, there are cases when the rectangular discretization does not work at all (see, for example, Ref. 5).

From the computational point of view, the use of the rectangular elements instead of an exact potential is something similar to calculating an integral by simple summation of the areas under the corresponding ladder steps. Even the trapezoidal rule is better and there are more accurate Simpson and Gaussian methods for evaluating integrals. A more accurate method for calculating the transfer matrix is needed as well. In Ref. 4 a trapezoidal approximation of the potential profile is employed (see also Ref. 6 and references therein). This undoubtedly improves the transfer matrix method, but the problem of discretization persists. Moreover an additional problem arises, namely, numerical evaluation of the Airy functions that are the exact solutions of the Schrödinger equation on the trapezoidal segments. In what follows, a new method that overcomes these difficulties is suggested.

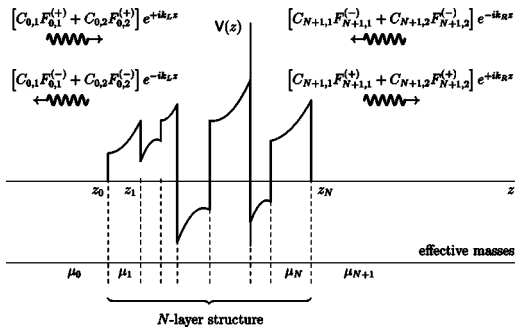


FIG. 2. An example of one-dimensional potential of a finite range outside of which ($z<z_0$ and $z>z_N$) the functions $F_{nj}^{(\pm)}(E,z)$ do not change with $z$ and therefore the physical wave function is reduced to the incoming and outgoing plane waves with the amplitudes given in the square brackets, and the asymptotic momenta $\hbar k_L=\sqrt{2\mu_0 E}$ and $\hbar k_R=\sqrt{2\mu_{N+1}E}$ determined by the total energy $E$. The combination coefficients $C_{0,j}$ and $C_{N+1,j}$ are related by the modified transfer matrix which is always a product of $(N+1)$ factors no matter how complicated $V(z)$ is inside each of the $N$ layers of the structure.

## III. MODIFIED TRANSFER MATRIX

In order to get rid of the rectangular discretization, let us first answer the question why the rectangular steps are needed in the standard transfer-matrix approach. There are two reasons for using the ladder approximation: Firstly, to easily obtain two linearly independent solutions (which simply are plane waves for the rectangular elements) of the Schrödinger equation on each interval of the potential constancy, and secondly, to have these solutions in the same explicit form (plane waves again) as the solutions have outside the interaction region. The second reason is more important because having the solutions in the form of plane waves on all the intermediate intervals makes it possible to relate the plane waves on the left and right ends of the structure by a $2\times 2$ matrix via a series of intermediate matchings.

The same can be achieved without the rectangular discretization, if we use the equations proposed in Ref. 5. To make the basic idea clear, let us first consider a simple case when the potential profile describing an $N$-layer nanostructure, has a finite range and is not biased, i.e., is zero for $z<z_0$ and $z>z_N$ as shown in Fig. 2. Let us also assume that the effective mass does not change within each physical layer, i.e., between $z_{n-1}$ and $z_n$. These simplifications are needed only to avoid cumbersome formulas that may compromise the clarity. A more general case is considered in the next section.

The points $z_0, z_1, \ldots, z_N$ divide the line $-\infty<z<+\infty$ in $N+2$ intervals (including two infinite intervals to the left and

to the right of the structure). Each of these intervals is uniquely identified by the subscript of its right border. Therefore, if formally $z_{-1}=-\infty$ and $z_{N+1}=+\infty$ then $z_{n-1}\leqslant z\leqslant z_n$ is the $n$th interval. Using the subscript $n$, we will label wave functions, effective masses, momenta etc., defined on the $n$th interval.

On each interval of the effective mass constancy $\mu(z)=\mu_n=\text{const}$ (in other words, inside each layer of the nanostructure), the Schrödinger equation (1) takes the form

$$\left(\frac{\hbar^2}{2\mu_n}\frac{d^2}{dz^2}+E\right)\psi(E,z)=\mathrm{V}(z)\psi(E,z). \tag{7}$$

As a differential equation of the second order, it has two linearly independent solutions that constitute the so-called fundamental system of solutions, from which any physical solution can be constructed as their linear combination. Let us look for these fundamental solutions, $\phi_{n1}(E,z)$ and $\phi_{n2}(E,z)$, in a special form that is convenient for constructing physical solutions with given asymptotic behavior. To this end, we can follow the idea of the variation parameters method (see, for example, Ref. 9).

In this method, one first finds two independent solutions of the homogeneous equation [when the right hand side of Eq. (7) is zero]. The general solution of the homogeneous equation is their linear combination with some constants (parameters). Then a solution of the total (nonhomogeneous) equation is sought in the form of the same combination but with the parameters considered as unknown functions of the independent variable.

In the case of Eq. (7), the plane waves $\exp(\pm ik_nz)$ with $k_n=\sqrt{2\mu_nE}/\hbar$ can be taken as the two independent solutions of the corresponding homogeneous equation. We, therefore, look for $\phi_{n1}(E,z)$ and $\phi_{n2}(E,z)$ in the following form

$$\phi_{n1}(E,z)=e^{ik_nz}F_{n1}^{(+)}(E,z)+e^{-ik_nz}F_{n1}^{(-)}(E,z),$$

$$\phi_{n2}(E,z)=e^{ik_nz}F_{n2}^{(+)}(E,z)+e^{-ik_nz}F_{n2}^{(-)}(E,z),\quad z\in[z_{n-1},z_n], \tag{8}$$

where $F_{n1}^{(\pm)}(E,z)$ and $F_{n2}^{(\pm)}(E,z)$ are unknown functions. When the potential vanishes, the functions $F_{nj}^{(\pm)}(E,z)$ become constants and therefore the form (8) ensures that our solutions have correct asymptotic behavior outside the interaction region. Furthermore, this behavior is given analytically which makes it easy to construct physical solutions with certain asymptotic boundary conditions (see Ref. 5).

Since instead of two unknown functions $\phi_{nj}, j=1, 2$, we introduce four unknown functions $F_{nj}^{(\pm)}$, they cannot be all independent. We, therefore, can impose two arbitrary conditions that relate them to each other. As such conditions, we choose the following two equations

$$e^{ik_nz}\partial_zF_{nj}^{(+)}(E,z)+e^{-ik_nz}\partial_zF_{nj}^{(-)}(E,z)=0,\quad j=1,2, \tag{9}$$

which are standard in the variation parameters method and are called the Lagrange conditions. Equations (9) simply mean that the first derivatives of $\phi_{nj}$ can be obtained by differentiation of the exponential factors only. This is used for deriving Eqs. (10) and further down in Eq. (17).

Substituting the ansatz (8) into the Schrödinger equation and using the conditions (9), we obtain a system of differential equations of the first order for the new unknown functions,

$$\partial_zF_{nj}^{(+)}(E,z)=\frac{e^{-ik_nz}}{2ik_n}V_n(z)[e^{ik_nz}F_{nj}^{(+)}(E,z)+e^{-ik_nz}F_{nj}^{(-)}(E,z)],$$

$$\partial_zF_{nj}^{(-)}(E,z)=-\frac{e^{ik_nz}}{2ik_n}V_n(z)[e^{ik_nz}F_{nj}^{(+)}(E,z)+e^{-ik_nz}F_{nj}^{(-)}(E,z)], \tag{10}$$

where $V_n(z)=(2\mu_n/\hbar^2)\mathrm{V}(z)$. It should be emphasized that this system is equivalent to the Schrödinger equation (7) from which we started. The subscript $j$ labels its two independent solutions on the $n$th interval, i.e., for $z\in[z_{n-1},z_n]$.

In any vector or functional space the choice of a basis is not unique. Our basis functions $\phi_{n1}(E,z)$ and $\phi_{n2}(E,z)$ can also be chosen in infinite number of ways by specifying the boundary conditions for them somewhere on the interval $[z_{n-1},z_n]$. The point $b_n\in[z_{n-1},z_n]$ where such conditions are imposed does not matter and, therefore, can be chosen to be convenient for calculations. Apparently, for numerical calculations, the most convenient point for imposing boundary conditions is one of the borders of the interval $[z_{n-1},z_n]$. On the leftmost and rightmost infinite intervals $[z_{-1},z_0]$ and $[z_N,z_{N+1}]$ the most convenient choice of $b_n$ is obvious, namely, $b_0=z_0$ and $b_{N+1}=z_N$.

Therefore, to guarantee linear independence of the basis solutions, we can use the following simple boundary conditions imposed on them at the right border of the leftmost interval and on the left borders of all the other intervals,

$$\phi_{n1}(E,b_n)=0,\quad \phi'_{n1}(E,b_n)=1,$$

$$\phi_{n2}(E,b_n)=1,\quad \phi'_{n2}(E,b_n)=0, \tag{11}$$

which imply that

$$F_{n1}^{(+)}(E,b_n)=\frac{e^{-ik_nb_n}}{2ik_n},\quad F_{n1}^{(-)}(E,b_n)=-\frac{e^{ik_nb_n}}{2ik_n},$$

$$F_{n2}^{(+)}(E,b_n)=\frac{e^{-ik_nb_n}}{2},\quad F_{n2}^{(-)}(E,b_n)=\frac{e^{ik_nb_n}}{2}, \tag{12}$$

where

$$b_n=\begin{cases}z_0, & n=0,\\ z_{n-1}, & n>0.\end{cases} \tag{13}$$

On each interval $z\in[z_{n-1},z_n]$, the physical solution $\psi_n(E,z)$ is a linear combination of the two basic solutions,

$$\psi_n(E,z)=C_{n1}\phi_{n1}(E,z)+C_{n2}\phi_{n2}(E,z). \tag{14}$$

Therefore, the physical wave function includes $N+2$ pairs of unknown combination coefficients $C_{n1}$ and $C_{n2}$. Of course, not all of them are independent. Indeed, at each of the $N+1$ matching points between adjacent intervals, the pairs of the constants $(C_{n1},C_{n2})$ and $(C_{n+1,1},C_{n+1,2})$ are subject to the

Ben-Daniel–Duke–Bastard matching conditions (5) and (6), namely,

$$\begin{pmatrix} \phi_{n1}(E,z_n) & \phi_{n2}(E,z_n) \\ \dfrac{\phi'_{n1}(E,z_n)}{\mu_n} & \dfrac{\phi'_{n2}(E,z_n)}{\mu_n} \end{pmatrix} \begin{pmatrix} C_{n1} \\ C_{n2} \end{pmatrix} = \begin{pmatrix} \phi_{n+1,1}(E,z_n) & \phi_{n+1,2}(E,z_n) \\ \dfrac{\phi'_{n+1,1}(E,z_n)}{\mu_{n+1}} & \dfrac{\phi'_{n+1,2}(E,z_n)}{\mu_{n+1}} \end{pmatrix} \begin{pmatrix} C_{n+1,1} \\ C_{n+1,2} \end{pmatrix}.$$

Similarly to the standard method, we see that they are related by a $2\times 2$ matrix,

$$\begin{pmatrix} C_{n1} \\ C_{n2} \end{pmatrix} = \mathcal{M}_{n,n+1} \begin{pmatrix} C_{n+1,1} \\ C_{n+1,2} \end{pmatrix}, \tag{15}$$

where

$$\begin{aligned} \mathcal{M}_{n,n+1} &= \begin{pmatrix} \phi_{n1}(E,z_n) & \phi_{n2}(E,z_n) \\ \dfrac{\phi'_{n1}(E,z_n)}{\mu_n} & \dfrac{\phi'_{n2}(E,z_n)}{\mu_n} \end{pmatrix}^{-1} \begin{pmatrix} \phi_{n+1,1}(E,z_n) & \phi_{n+1,2}(E,z_n) \\ \dfrac{\phi'_{n+1,1}(E,z_n)}{\mu_{n+1}} & \dfrac{\phi'_{n+1,2}(E,z_n)}{\mu_{n+1}} \end{pmatrix} = \begin{pmatrix} \phi_{n1}(E,z_n) & \phi_{n2}(E,z_n) \\ \dfrac{\phi'_{n1}(E,z_n)}{\mu_n} & \dfrac{\phi'_{n2}(E,z_n)}{\mu_n} \end{pmatrix}^{-1} \begin{pmatrix} 0 & 1 \\ \frac{1}{\mu_{n+1}} & 0 \end{pmatrix} \\ &= \begin{pmatrix} \frac{\mu_{n+1}}{\mu_n}\phi'_{n1}(E,z_n) & \frac{\mu_{n+1}}{\mu_n}\phi'_{n2}(E,z_n) \\ \phi_{n1}(E,z_n) & \phi_{n2}(E,z_n) \end{pmatrix}^{-1} \end{aligned} \tag{16}$$

which can be called the modified transfer matrix. As a result of having $N+1$ relations of the type (15), we remain with only one unknown pair of the combination coefficients. This "free" pair, $(C_{01},C_{02})$ or $(C_{N+1,1},C_{N+1,2})$, has to be chosen to satisfy the asymptotic physical boundary conditions at large $|z|$ (bound, resonant, or scattering state conditions), while all the other coefficients are obtained with the help of the modified transfer matrices (16) via the relation (15).

The elements of the transfer matrix (16), involving

$$\phi_{nj}(E,z_n) = e^{ik_n z_n} F_{nj}^{(+)}(E,z_n) + e^{-ik_n z_n} F_{nj}^{(-)}(E,z_n)$$

and

$$\phi'_{nj}(E,z_n) = ik_n[e^{ik_n z_n} F_{nj}^{(+)}(E,z_n) - e^{-ik_n z_n} F_{nj}^{(-)}(E,z_n)], \quad j=1,2, \tag{17}$$

for $n>0$ can be obtained by numerically solving the differential equations (10) from $z_{n-1}$ to $z_n$ with the initial conditions (12). The transfer matrix $\mathcal{M}_{0,1}$ for the leftmost matching point is calculated without solving the differential equations because for both adjacent intervals the boundary conditions are imposed at the same point. It follows from Eq. (16) that

$$\mathcal{M}_{0,1} = \begin{pmatrix} \frac{\mu_0}{\mu_1} & 0 \\ 0 & 1 \end{pmatrix}. \tag{18}$$

The total transfer-matrix $\mathcal{K}$ that relates the combination coefficients at the left and right hand sides of the physical structure,

$$\begin{pmatrix} C_{0,1} \\ C_{0,2} \end{pmatrix} = \mathcal{K} \begin{pmatrix} C_{N+1,1} \\ C_{N+1,2} \end{pmatrix}. \tag{19}$$

is a product of the elementary matrices,

$$\mathcal{K} = \mathcal{M}_{0,1}\mathcal{M}_{1,2}\mathcal{M}_{2,3}\ldots\mathcal{M}_{N-1,N}\mathcal{M}_{N,N+1}. \tag{20}$$

The idea of constructing the physical wave function on each interval of the effective mass constancy as a linear combination of two independent solutions was used before in Ref. 4. Formally, the authors of Ref. 4 consider an arbitrary potential profile and derive for it the so-called propagation matrix in the form of a Wick expansion. However, in practical calculations they have to discretize the profile in thin elements and find two independent solutions of the Schrödinger equation on each of these elements analytically. This of course is only possible in a limited number of special cases. They consider two simple cases, namely, rectangular and trapezoidal elements. For the general case, they use the WKB solutions.

The difference of the modified transfer matrix method from the standard one consists in the fact that we do not discretize the potential profile. As a result the number of factors in the product (20) is always equal to the number of intervals where the effective mass has different values, plus one, that is to the number of different physical layers in the nanostructure plus one, no matter how complicated the potential profile is. To obtain these factors, we only need to numerically solve differential equations (10) on the corresponding intervals.

There is another difference: The modified transfer matrix relates not the amplitudes of the plane waves but the combination coefficients that form physical solution out of the two independent solutions. Although this may look like a complication, in fact, it is an advantage that enables us to construct the Jost matrices which are very important quantities of formal scattering theory.

In the multichannel scattering theory (see, for example, Ref. 10), the Jost matrices are defined via the asymptotic behavior of the general solution of Schrödinger equation. Every particular solution of an $N$-channel Schrödinger equation is a column that consists of $N$ rows each describing the

motion in one of the $N$ channels. The general solution $\Phi(E,r)$ is a square matrix

$$\Phi(E,r)=\begin{pmatrix}\varphi_{11}(E,r) & \varphi_{12}(E,r) & \dots & \varphi_{1N}(E,r)\\ \varphi_{21}(E,r) & \varphi_{22}(E,r) & \dots & \varphi_{2N}(E,r)\\ \vdots & \vdots & \vdots & \vdots\\ \varphi_{N1}(E,r) & \varphi_{N2}(E,r) & \dots & \varphi_{NN}(E,r)\end{pmatrix},$$

that combines all linearly independent columns each representing a particular solution. Far away from the interaction region (i.e., when $r\to\infty$), in all the columns the wave function in each channel is a linear combination of the incoming and outgoing plane waves and, therefore,

$$\Phi(E,r)\underset{r\to\infty}{\to}\mathcal{W}^{(\mathrm{in})}(r)f^{(\mathrm{in})}(E)+\mathcal{W}^{(\mathrm{out})}(r)f^{(\mathrm{out})}(E),$$

where $\mathcal{W}^{(\mathrm{in})}(r)$ and $\mathcal{W}^{(\mathrm{out})}(r)$ are the diagonal matrices

$$\mathcal{W}^{(\mathrm{in/out})}(r)=\begin{pmatrix}e^{\mp ik_1 r} & 0 & \dots & 0\\ 0 & e^{\mp ik_2 r} & \dots & 0\\ \vdots & \vdots & \vdots & \vdots\\ 0 & 0 & \dots & e^{\mp ik_N r}\end{pmatrix},$$

of the plane waves with the corresponding channel momenta $k_j$. The $N\times N$ matrices $f^{(\mathrm{in/out})}(E)$, called the Jost matrices, consist of the asymptotic combination coefficients. They completely determine the spectral and scattering properties of a given multi-channel potential. It can be shown, that the $S$ matrix is the product

$$S(E)=f^{(\mathrm{out})}(E)[f^{(\mathrm{in})}(E)]^{-1}, \tag{21}$$

and the spectral points (bound and resonant states) are complex roots $E=E_r-i\Gamma/2$ of the equation

$$\det f^{(\mathrm{in})}(E)=0. \tag{22}$$

This theory is relevant to the motion of a particle on an infinite line since this motion is inherently a multichannel problem that has at least two channels involved. These two channels are the motion on the left and right halves of the line. Formal consideration of a one-dimensional problem as a two-channel one and a definition of the corresponding Jost matrices in terms of the asymptotics of the general solution of one-dimensional Schrödinger equation, consistent with the standard three-dimensional multi-channel theory, is given in the Appendix (see also the discussion in Ref. 5).

In order to obtain the Jost matrix $f^{(\mathrm{in})}$, using the modified transfer matrix, we recall that the spectral points (bound or resonant states) are those points of the complex energy plane at which the wave function has only outgoing waves in the asymptotic regions. Therefore, for spectral points, the amplitudes of the incoming waves at the left and right ends of the line (see Fig. 2) must be zero,

$$C_{0,1}F^{(+)}_{0,1}(E,-\infty)+C_{0,2}F^{(+)}_{0,2}(E,-\infty)=0,$$

$$C_{N+1,1}F^{(-)}_{N+1,1}(E,+\infty)+C_{N+1,2}F^{(-)}_{N+1,2}(E,+\infty)=0. \tag{23}$$

In this linear system, $F$'s are calculated values and $C$'s are unknowns. Using Eq. (19), the left-end combination coefficients $C_{0,1}$ and $C_{0,2}$ can be expressed in terms of the corresponding coefficients at the right end via the modified transfer matrix $\mathcal{K}$,

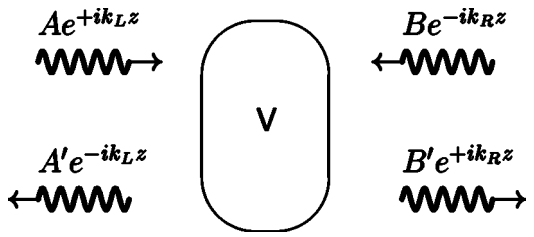


FIG. 3. Schematic picture of the scattering process with $A$ and $B$ being amplitudes of the incident and $A'$ and $B'$ of the scattered waves in the left and right channels with the channel momenta $k_L$ and $k_R$, respectively.

$$C_{0j}=\mathcal{K}_{j1}C_{N+1,1}+\mathcal{K}_{j2}C_{N+1,2},\quad j=1,2. \tag{24}$$

As was said before, we remain with one pair of "free" (unknown) coefficients $C_{N+1,1}$ and $C_{N+1,2}$ that can be found from a homogeneous system of linear equations (23). This system may have nontrivial solutions if and only if its determinant is zero, i.e., when Eq. (22) holds with the Jost matrix defined as

$$f^{(\mathrm{in})}(E)\equiv\begin{pmatrix}\mathcal{K}_{11}F^{(+)}_{0,1}+\mathcal{K}_{21}(E)F^{(+)}_{0,2} & \mathcal{K}_{12}F^{(+)}_{0,1}+\mathcal{K}_{22}F^{(+)}_{0,2}\\ F^{(-)}_{N+1,1} & F^{(-)}_{N+1,2}\end{pmatrix}. \tag{25}$$

It should be remembered that all $\mathcal{K}$'s and $F$'s depend on the energy $E$. We drop their arguments for the sake of notation simplicity. Formally, $F^{(+)}_{0,j}$ in Eq. (25) should be taken at the far left end $(-\infty)$ and $F^{(-)}_{N+1,j}$ at the far right end $(+\infty)$ of the line, but they actually do not depend on $z$ because the potential is zero for $z<z_0$ and $z>z_N$.

For a scattering process schematically presented in Fig. 3, the $S$ matrix relates the amplitudes $A$ and $B$ of the incoming waves in the left and right channels with the corresponding outgoing wave amplitudes $A'$ and $B'$, viz.

$$\begin{pmatrix}A'\\ B'\end{pmatrix}=S\begin{pmatrix}A\\ B\end{pmatrix}. \tag{26}$$

Comparing the plane-wave amplitudes given in Figs. 2 and 3, we see that

$$C_{0,1}F^{(+)}_{0,1}+C_{0,2}F^{(+)}_{0,2}=A,$$

$$C_{N+1,1}F^{(-)}_{N+1,1}+C_{N+1,2}F^{(-)}_{N+1,2}=B,$$

$$C_{0,1}F^{(-)}_{0,1}+C_{0,2}F^{(-)}_{0,2}=A',$$

$$C_{N+1,1}F^{(+)}_{N+1,1}+C_{N+1,2}F^{(+)}_{N+1,2}=B'. \tag{27}$$

Using Eq. (24) and defining the "out" Jost matrix as

$$f^{(\mathrm{out})}(E)\equiv\begin{pmatrix}\mathcal{K}_{11}F^{(-)}_{0,1}+\mathcal{K}_{21}F^{(-)}_{0,2} & \mathcal{K}_{12}F^{(-)}_{0,1}+\mathcal{K}_{22}F^{(-)}_{0,2}\\ F^{(+)}_{N+1,1} & F^{(+)}_{N+1,2}\end{pmatrix}, \tag{28}$$

we can divide the system (27) of four equations in the following two pairs

$$f^{(\mathrm{in})}(E)\begin{pmatrix} C_{N+1,1} \\ C_{N+1,2} \end{pmatrix} = \begin{pmatrix} A \\ B \end{pmatrix} \tag{29}$$

and

$$f^{(\mathrm{out})}(E)\begin{pmatrix} C_{N+1,1} \\ C_{N+1,2} \end{pmatrix} = \begin{pmatrix} A' \\ B' \end{pmatrix}, \tag{30}$$

from which Eq. (21) immediately follows.

Therefore the spectral points can be found from Eq. (22) and the scattering parameters (transmission and reflection coefficients that constitute the $S$ matrix as described in the Appendix) from Eq. (21). This means that the definitions (25) and (28) of the Jost matrices in terms of the modified transfer matrix are consistent with general multichannel theory.

Within the proposed scheme, we can obtain a complete solution of the one-dimensional problem. Indeed, in addition to the spectral points and the scattering parameters, we always have the physical wave function as a by-product, which is constructed (for each interval) as linear combination of the two independent solutions. The scattering wave function thus constructed, is automatically normalized to the incoming flux $|A|^2+|B|^2$. For example, if we choose $A=1$ and $B=0$, the wave function will describe the probability density distribution for a unit flux falling from the left. The wave function of a bound state should be normalized to 1 in the usual way, i.e., by calculating the normalization integral over the entire $z$-line.

There is another feature that makes the proposed method different from the traditional transfer matrix approach. This is a simple and accurate way of calculating not only total width of a resonance but its partial widths as well. In formal multi-channel scattering theory, it is shown (see the Appendix and Ref. 5) that in a vicinity of an isolated resonance the $S$-matrix has the following form

$$S(E) = \mathrm{const} \times \left[ 1 - \frac{i}{E - E_r + i\Gamma/2} \begin{pmatrix} \Gamma_L & \sqrt{\Gamma_L \Gamma_R} \\ \sqrt{\Gamma_R \Gamma_L} & \Gamma_R \end{pmatrix} \right],$$

where $|\mathrm{const}|=1$ and the total width $\Gamma=\Gamma_L+\Gamma_R$ is a sum of the partial widths. The ratio of a partial width to the total width gives relative probability that the resonance will decay in a particular channel. This form of the $S$-matrix offers a simple way of calculating the partial widths $\Gamma_L$ and $\Gamma_R$ as the limits

$$\Gamma_\ell = \lim_{E \to (E_r - i\Gamma/2)} \left| (E - E_r + i\Gamma/2) S_{\ell\ell}(E) \right|, \quad \ell = L, R.$$

In practical calculations, however, this procedure may cause numerical instabilities since the $S$-matrix is singular at the resonance energy. To avoid this difficulty, we can use the fact that the sum $\Gamma$ of the partial widths is obtained simultaneously with the resonance energy $E_r$ when Eq. (22) is solved. What remains is to find the ratio

$$\frac{\Gamma_L}{\Gamma_R} = \lim_{E \to (E_r - i\Gamma/2)} \left| \frac{S_{LL}(E)}{S_{RR}(E)} \right| = \left| \frac{f_{11}^{(\mathrm{out})} f_{22}^{(\mathrm{in})} - f_{12}^{(\mathrm{out})} f_{22}^{(\mathrm{in})}}{f_{22}^{(\mathrm{out})} f_{11}^{(\mathrm{in})} - f_{21}^{(\mathrm{out})} f_{12}^{(\mathrm{in})}} \right|_{E = E_r - i\Gamma/2}$$

where the vanishing denominators of $S_{LL}$ and $S_{RR}$ (determinant of the Jost matrix) cancel out.

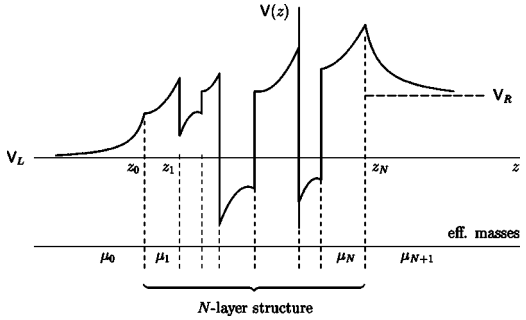


FIG. 4. An example of biased one-dimensional potential with the tails extending to infinity in both directions. The asymptotic values $V_L$ and $V_R$ of the tails are the threshold energies for the left and right channels.

## IV. MODIFIED TRANSFER MATRIX: GENERAL CASE

In the previous section, for the sake of clarity, certain simplifications were used, namely, it was assumed that the potential was of a finite range and not biased (i.e., had the same value on both sides of the structure). Here these assumptions are revoked. Let us consider a more general case when on both sides of the $z$-line the potential gradually tends to its asymptotic values $V_L$ and $V_R$ (see Fig. 4) which are different threshold energies for the left and right channels.

We assume that the potential $V(z)$ tends to the asymptotic constants faster than $|z|^{-1}$, i.e.,

$$\lim_{z \to \pm\infty} z[V(z) - V_{R,L}] = 0. \tag{31}$$

Possible Coulombic tails

$$V^c(z) = \begin{cases} Q_L/z, & z < z_0, \\ 0, & z_0 \leqslant z \leqslant z_N, \\ Q_R/z, & z > z_N, \end{cases} \tag{32}$$

that may be present on one or both sides of the structure due to the charge accumulation on its surfaces, can always be separated from the short-range part $V(z)$ of the total potential energy, by adding and subtracting $V^c(z)$. Therefore, in general the total potential is the sum $V(z)+V^c(z)$ and the effective-mass Schrödinger equation has the form

$$\left[ -\frac{\hbar^2}{2} \frac{d}{dz} \frac{1}{\mu(z)} \frac{d}{dz} + V(z) + V^c(z) - E \right] \psi(E,z) = 0. \tag{33}$$

Within each interval $[z_{n-1}, z_n]$ of the effective-mass constancy, this equation takes a more simple form

$$\left[ \frac{d^2}{dz^2} + k_n^2 - V_n^c(z) \right] \psi(E,z) = V_n(z) \psi(E,z), \tag{34}$$

where by adding and subtracting the threshold energy $V_L$ or $V_R$, we introduce the channel momentum on the $n$th interval

$$\hbar k_n = \begin{cases} \sqrt{2\mu_n (E - V_L)}, & z_n \leqslant 0, \\ \sqrt{2\mu_n (E - V_R)}, & z_n > 0, \end{cases} \tag{35}$$

and the renormalized potentials

$$V_n^c(z) = \frac{2\mu_n}{\hbar^2}\mathsf{V}^c(z) \tag{36}$$

and

$$V_n(z) = \begin{cases} \dfrac{2\mu_n}{\hbar^2}[\mathsf{V}(z) - \mathsf{V}_L], & z_n \leqslant 0, \\ \dfrac{2\mu_n}{\hbar^2}[\mathsf{V}(z) - \mathsf{V}_R], & z_n > 0. \end{cases} \tag{37}$$

According to condition (31), the right-hand side of Eq. (34) vanishes when $|z| \to \infty$, faster than the Coulomb tails (36). Therefore, far away from the interaction region, Eq. (34) is reduced to

$$\left(\frac{d^2}{dz^2} + k_n^2 - \frac{2\eta_n k_n}{z}\right)\psi(E,z) = 0, \quad |z| \to \infty, \tag{38}$$

where the Coulomb parameter $\eta_n$ for the $n$th interval is defined in the standard way,

$$\eta_n = \frac{\mu_n Q_n}{\hbar^2 k_n}, \tag{39}$$

and, in accordance with Eq. (32), $Q_0 = Q_L, Q_1 = Q_2 = \cdots = Q_N = 0, Q_{N+1} = Q_R$. Two independent solutions of Eq. (38) are the standard Coulomb functions (see, for example, Ref. 11) with zero angular momentum, namely, the regular $\mathcal{F}_0(\eta_n, k_n z)$ and irregular $\mathcal{G}_0(\eta_n, k_n z)$ Coulomb functions. These functions are normalized in such a way that, when the Coulomb parameter is zero, they are reduced to the trigonometric functions, $\mathcal{F}_0(0,\zeta) = \sin\zeta$ and $\mathcal{G}_0(0,\zeta) = \cos\zeta$. Their linear combinations

$$\mathcal{H}_0^{(\pm)}(\eta,\zeta) \equiv \mathcal{G}_0(\eta,\zeta) \pm i\mathcal{F}_0(\eta,\zeta), \tag{40}$$

are more convenient for the purpose of using the variation of parameters method. Indeed, they are two independent solutions of the homogeneous equation (38) as well, and when $\eta \to 0$ (no charge) they are smoothly transformed into ordinary plane waves,

$$\mathcal{H}_0^{(\pm)}(\eta,\zeta) \underset{\eta\to 0}{\to} e^{\pm i\zeta}. \tag{41}$$

In the general case when $\eta \neq 0$, far away from the interaction region, functions (40) become the Coulomb-modified plane waves,

$$\mathcal{H}_0^{(\pm)}(\eta,\zeta) \underset{|\zeta|\to\infty}{\to} \exp\{\pm i[\zeta - \eta \ln 2\zeta + \arg\Gamma(1 + i\eta)]\}, \tag{42}$$

that should be used instead of ordinary plane waves whenever a Coulomb potential is involved because it falls off so slowly that the particle feels its influence even when moves far away (see, for example, Ref. 10). Therefore, generalizing Eq. (8), we look for two linearly independent solutions of Eq. (34) on the interval $z \in [z_{n-1}, z_n]$ in the following form

$$\phi_{n1}(E,z) = \mathcal{H}_0^{(+)}(\eta_n,k_n z)F_{n1}^{(+)}(E,z) + \mathcal{H}_0^{(-)}(\eta_n,k_n z)F_{n1}^{(-)}(E,z),$$

$$\phi_{n2}(E,z) = \mathcal{H}_0^{(+)}(\eta_n,k_n z)F_{n2}^{(+)}(E,z) + \mathcal{H}_0^{(-)}(\eta_n,k_n z)F_{n2}^{(-)}(E,z). \tag{43}$$

Then, with the Lagrange condition

$$\mathcal{H}_0^{(+)}(\eta_n,k_n z)\partial_z F_{nj}^{(+)}(E,z) + \mathcal{H}_0^{(-)}(\eta_n,k_n z)\partial_z F_{nj}^{(-)}(E,z) = 0, \quad j = 1,2, \tag{44}$$

Eq. (34) is transformed into a system of the first-order equations

$$\partial_z F_{nj}^{(+)}(E,z) = \frac{\mathcal{H}_0^{(-)}(\eta_n,k_n z)}{2ik_n}V_n(z)[\mathcal{H}_0^{(+)}(\eta_n,k_n z)F_{nj}^{(+)}(E,z) + \mathcal{H}_0^{(-)}(\eta_n,k_n z)F_{nj}^{(-)}(E,z)],$$

$$\partial_z F_{nj}^{(-)}(E,z) = -\frac{\mathcal{H}_0^{(+)}(\eta_n,k_n z)}{2ik_n}V_n(z)[\mathcal{H}_0^{(+)}(\eta_n,k_n z)F_{nj}^{(+)}(E,z) + \mathcal{H}_0^{(-)}(\eta_n,k_n z)F_{nj}^{(-)}(E,z)]. \tag{45}$$

The boundary conditions defining two pairs of independent solutions of this system, follow from Eqs. (11)

$$F_{n1}^{(+)}(E,b_n) = \frac{\mathcal{H}_0^{(-)}(\eta_n,k_n b_n)}{2ik_n}, \quad F_{n1}^{(-)}(E,b_n) = -\frac{\mathcal{H}_0^{(+)}(\eta_n,k_n b_n)}{2ik_n},$$

$$F_{n2}^{(+)}(E,b_n) = -\frac{\mathcal{H}_0'^{(-)}(\eta_n,k_n b_n)}{2i}, \quad F_{n2}^{(-)}(E,b_n) = \frac{\mathcal{H}_0'^{(+)}(\eta_n,k_n b_n)}{2i}, \tag{46}$$

where, as before, $b_n$ is given by Eq. (13), i.e., is the right border for the leftmost interval and left border for all the other intervals. Here $\mathcal{H}_0'^{(\pm)}(\eta,\zeta) \equiv \partial_\zeta \mathcal{H}_0^{(\pm)}(\eta,\zeta)$ and we used known value of the Wronskian $\mathcal{F}_0'\mathcal{G}_0 - \mathcal{F}_0\mathcal{G}_0' = 1$ of the standard Coulombic functions. As can be easily checked, these boundary conditions are transformed into (12) when $\eta_n \to 0$. Perhaps it should be emphasized that the Coulomb interaction only needs to be separated from the total potential on the leftmost ($n=0$) and rightmost ($n=N+1$) intervals of the line, i.e., we can always assume that $\eta_1 = \eta_2 = \cdots = \eta_N = 0$. According to Eq. (41), this means that for $n = 1,2,\ldots,N$ the Coulombic functions $\mathcal{H}_0^{(\pm)}(\eta_n,k_n z)$ in the system (45) can be replaced with the plane waves.

Therefore the procedure of finding physical wave function (14) on the inner intervals and the elementary transfer matrices (16) is basically the same as was described in Sec. III. The only difference here is that the momentum (35) and the potential (37) on the left and right halves of the line, are shifted by (generally) unequal thresholds $\mathsf{V}_L$ and $\mathsf{V}_R$. In numerical calculations it is important to remember that when taking complex square root in Eq. (35), we must choose such sign in front of it that imaginary part of the momentum is positive for a closed channel and negative for an open one. This corresponds to the choice between the physical and unphysical sheets of the Riemann $E$ surface (see Ref. 5) and ensures correct asymptotic behavior of the wave function.

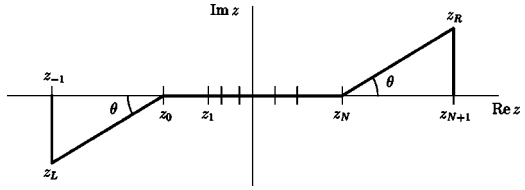


FIG. 5. Deformed integration path for solving Eqs. (45) with a potential having the tails that extend to infinity, for complex energies $E=E_R-iE_I$ from the resonance domain.

The total transfer matrix $\mathcal{K}$ is not sufficient to construct the physical wave function and Jost matrices. What we need else, are the solutions $F_{nj}^{(\pm)}(E,z)$ of Eqs. (45) on the outer intervals $z<z_0$ and $z>z_N$. With the potential tails extending to infinity, these intervals may require a special treatment.

As was shown in Ref. 5, when the bound and scattering states are considered, the solutions of Eqs. (45) always converge to the limit values $F_{0,j}^{(\pm)}(E,-\infty)$ and $F_{N+1,j}^{(\pm)}(E,+\infty)$. The resonances require a bit more sophisticated approach. Although these limits always exist, the solutions of Eqs. (45) for complex energies do not, in general, converge to them along the $z$-line. We can, however, obtain converging results for the limits $\lim_{|z|\to\infty}F_{nj}^{(\pm)}(E,z)$ if go towards the infinity along a deformed path in the complex coordinate plane. In Ref. 5 it was shown that $F_{nj}^{(-)}(E,z)$ converges if at long distances the integration path is such that $\mathrm{Im}\, k_\ell z\geqslant 0$, where $k_\ell$ is the corresponding asymptotic channel-momentum ($k_L=k_0$ for the left and $k_R=k_{N+1}$ for the right channel), while $F_{nj}^{(+)}(E,z)$ attains its finite limit along a path with $\mathrm{Im}\, k_\ell z\leqslant 0$.

Therefore, when doing the calculations at complex energies $E=E_1-iE_2$ in the resonance domain, the convergence can be achieved by integrating Eqs. (45) along the path shown in Fig. 5, where the angle $\theta$ should be chosen large enough and positive for obtaining $f^{(\mathrm{in})}(E)$ and negative for calculating $f^{(\mathrm{out})}(E)$. Indeed, according to the definitions (25) and (28), the matrix elements of $f^{(\mathrm{in})}(E)$ involve $F_{nj}^{(+)}(E,z)$ at the far left and $F_{nj}^{(-)}(E,z)$ at the far right end of the line, while for the matrix $f^{(\mathrm{out})}(E)$ the situation is just opposite. If the asymptotic channel-momenta, corresponding to the energy $E=E_1-iE_2$, are $k_\ell=|k_\ell|\exp(-i\omega_\ell)$ then on the inclined segments of the path where

$$z=\begin{cases} z_0-r\exp(i\theta) & \text{for the leftmost segment,}\\ z_N+r\exp(i\theta) & \text{for the rightmost segment.}\end{cases} \tag{47}$$

we have

$$\mathrm{Im}\, k_\ell z=\begin{cases} -|k_L|[r\sin(\theta-\omega_L)+z_0\sin\omega_L], & \ell=L,\\ +|k_R|[r\sin(\theta-\omega_R)-z_N\sin\omega_R], & \ell=R.\end{cases} \tag{48}$$

From Eq. (48) it is clear that with positive $\theta>\omega_\ell$, we can always find such value $r_m$ that for all $r>r_m$ the above mentioned necessary conditions for the convergence of all matrix elements of $f^{(\mathrm{in})}(E)$ are fulfilled. Similarly, the convergence conditions for $f^{(\mathrm{out})}(E)$ can be fulfilled with $\theta\leqslant 0$. On vertical segments $[z_{-1},z_L]$ and $[z_R,z_{N+1}]$ the functions $F_{nj}^{(\pm)}(E,z)$ do not change because the potential vanishes making the right-hand sides of Eqs. (45) infinitesimal. In the calculations we, therefore, can simply ignore these segments assuming that the points $z_{-1}$ and $z_{N+1}$ are shifted to $z_L$ and $z_R$, respectively.

As a final note, perhaps it should be mentioned that the left and right outer intervals can be treated differently. The rotation angle $\theta$ for them should not necessarily be the same as well as the lengths of the inclined line segments. Furthermore, the boundary conditions that make the solutions $\phi_{n1}(E,z)$ and $\phi_{n2}(E,z)$ linearly independent on the interval $[z_n,z_{n+1}]$ can differ from (11). Their choice is certainly not unique. Any other conditions that guarantee the solution independence can be used as well. As can be easily seen, the choice of these conditions changes the values of $f^{(\mathrm{in})}(E)$ and $f^{(\mathrm{out})}(E)$. Since, however, the equations defining $F_{nj}^{(\pm)}(E,z)$ are linear and homogeneous, they change in such a way that both acquire a common factor which cancels out when the $S$ matrix and the ratio $\Gamma_L/\Gamma_R$ are calculated. This factor is similar to the wave function normalization and does not affect any observable quantities.

## V. NUMERICAL EXAMPLES

The modified transfer matrix method developed in the preceding sections, should work equally well when the effective masses are the same on all the segments $[z_{n-1},z_n]$. The first test calculations were, therefore, performed for the potentials used in Ref. 5 where the Jost function method based on Eqs. (10) was applied to the problems with constant effective mass. As was expected, the tests showed that the results did not depend on the the way the potential profile was divided in segments. All the numbers obtained in Ref. 5, were reproduced with the modified transfer matrix method to the same accuracy and, therefore, are not given in the present publication once again. Instead, three new examples are considered. For the first of them, the results of calculations based on the traditional transfer matrix method are available, and for the last one, the exact solutions are known.

### A. Biased AlInAs/GaInAs nanostructure

In Ref. 12, a nanostructure consisting of an alternating sequence (4.5 nm−0.8 nm−3.5 nm−3.5 nm−3.0 nm

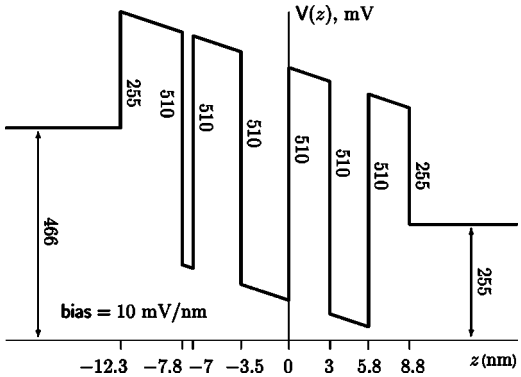


FIG. 6. Biased AlInAs/GaInAs nanostructure of Ref. 12. The effective mass is $0.072m_e$, $0.043m_e$, and $0.0575m_e$ inside the barriers, wells, and the external regions, respectively.

TABLE I. Lowest part of the resonance spectrum for an electron moving in the biased AlInAs/GaInAs nanostructure which is modeled by the potential given in Fig. 6. The results obtained within the APM, PWM, RCP, and RCD methods are taken from Ref. 12.

| $E$ (meV) | $\tau$ (ps) | $\Gamma_L$ (meV) | $\Gamma_R$ (meV) | Method |
|---|---|---|---|---|
| 263.763 460 796 7 | 0.505 637 819 0 | 0 | 1.301 746 379 1 | this work |
| 263.77 | 0.51 | | | APM |
| 263.80 | 0.50 | | | PWM |
| 263.76 | 0.50 | | | RCP(R) |
| 263.78 | 0.49 | | | RCD(M) |
| 263.76 | 0.50 | | | RCD(QRPM) |
| 297.165 851 614 5 | 0.659 920 930 2 | 0 | 0.997 410 704 7 | this work |
| 297.17 | 0.66 | | | APM |
| 297.15 | 0.66 | | | PWM |
| 297.17 | 0.66 | | | RCP(R) |
| 297.16 | 0.66 | | | RCD(M) |
| 297.17 | 0.66 | | | RCD(QRPM) |
| 615.522 237 975 0 | 0.101 359 540 5 | 6.185 771 358 7 | 0.308 064 314 4 | this work |
| 615.54 | 0.10 | | | APM |
| 615.66 | 0.10 | | | PWM |
| 615.69 | 0.28 | | | RCP(R) |
| 615.56 | 0.11 | | | RCP(L) |
| 615.78 | 0.11 | | | RCD(M) |
| 615.54 | 0.10 | | | RCD(QRPM) |
| 750.812 982 655 7 | 0.018 247 088 7 | 3.761 555 840 7 | 32.310 620 404 2 | this work |
| 750.82 | 0.02 | | | APM |
| 750.23 | 0.02 | | | PWM |
| 752.19 | 0.02 | | | RCP(R) |
| 753.86 | 0.07 | | | RCP(L) |
| 755.20 | 0.02 | | | RCD(M) |
| 750.97 | 0.02 | | | RCD(QRPM) |
| 877.687 119 644 4 | 0.004 323 227 1 | 9.481 925 500 5 | 142.768 278 403 4 | this work |
| 975.916 495 779 6 | 0.003 087 180 9 | 93.364 682 653 7 | 119.843 492 437 7 | this work |
| 1129.138 363 768 8 | 0.002 625 098 8 | 23.292 728 993 6 | 227.445 337 135 8 | this work |

$-2.8$ nm $-3.0$ nm) of AlInAs and GaInAs semiconductor layers is modeled by a rectangular potential profile. The barriers of this profile represent the AlInAs layers and all have the height of 510 meV with the effective mass $\mu=0.072\ m_e$, where $m_e$ is the free electron mass. The zero height wells represent the GaInAs layers with $\mu=0.043\ m_e$. The external thick layers are assumed to be an equal proportion mixture of AlInAs and GaInAs and, therefore, have the conduction potential of 255 meV and $\mu=0.0575\ m_e$. The nanostructure is biased by 10 mV/nm. The resulting potential profile is shown in Fig. 6.

The lowest part of the resonance spectrum generated by this potential is given in Table I where our results are compared with the corresponding resonance parameters obtained in Ref. 12 by different methods, namely, by the argument principle method (APM), the perturbed wave number method (PWM), two reflection coefficient phase methods [RCP(R) and RCP(L)], and two reflection coefficient denominator methods [RCD(M) and QRPM]. For the sake of comparison, total widths of the resonances are given in terms of the corresponding lifetimes $\tau=\hbar/\Gamma$ as was done in Ref. 12. The partial widths $\Gamma_L$ and $\Gamma_R$ that determine relative probabilities $\Gamma_L/\Gamma$ and $\Gamma_R/\Gamma$ of resonance decaying into the left and right channels, are not given in Ref. 12.

Since there is no rectangular discretization or any other approximation in our approach, it gives the results whose accuracy is limited only by the computer round-off's and the tolerance requested from the routine that numerically solves differential equations. We therefore assume that the correct digits in the calculated resonance energies are those which do not change when the same root of Eq. (22) is found by the Newton method, starting from different initial points in the complex energy plane. This assumption proved to be correct when we tested our method using potentials with analytically known solutions (see example A of Ref. 5 and Sec. V C of the present paper). Although our results are given in Table I with ten digits after decimal point, actual accuracy of the calculations was even higher. As is seen, the rectangular discretization used in the standard transfer matrix approach is

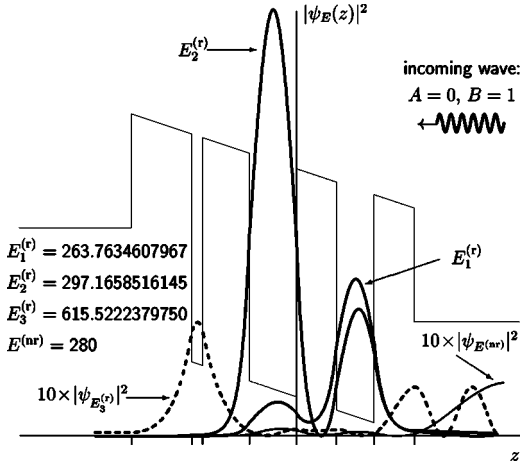


FIG. 7. Electron density distribution in the biased AlInAs/GaInAs nanostructure of Ref. 12 for four energies of the plane wave falling from the right with unit amplitude.

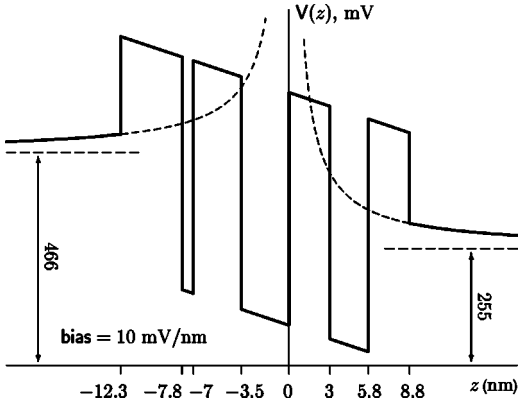


FIG. 8. Biased AlInAs/GaInAs nanostructure of Ref. 12, modified by addition of the Coulombic tails (32) on both its sides with $Q_R=-Q_L=500$ mV nm.

not harmless. It limits the accuracy of all the results of Ref. 12 to four or even three correct digits.

Figure 7 shows the probability density distribution inside the nanostructure for electron plane waves of unit amplitude incoming from the right [$A=0$ and $B=1$ in Eq. (26), see also Fig. 3] with three resonant ($E_1^{(r)}=263.763\,460\,796\,7$ meV, $E_2^{(r)}=297.165\,851\,614\,5$ meV, $E_3^{(r)}=615.522\,237\,975\,0$ meV) and one nonresonant ($E^{(\mathrm{nr})}=280$ meV) energies. These curves clearly demonstrate a tendency towards localization when the scattering is resonant, which becomes more pronounced for narrow resonances.

### B. Biased AlInAs/GaInAs nanostructure with Coulombic tails

Let us modify the potential of the previous example by adding to it the Coulombic tails (32) that begin on the left and right borders of the nanostructure and extend to infinity in both directions. For $Q_R=-Q_L=500$ mV nm, the resulting potential is shown in Fig. 8 and several states of the corresponding resonance spectrum are given in Table II.

Comparing Tables I and II, we see that even relatively weak tails significantly change the lifetimes of low-lying resonances. For the higher resonances, the energies and total widths are shifted only slightly but the distribution of the decay probabilities between the left and right channels is notably different. Very fast (exponential) growth of the lifetime of the lowest resonance when the strength $Q=Q_R=-Q_L$ of the tails is increased from zero to 500mV·nm, is shown in Fig. 9. Such dramatic variations of the resonance lifetime even with small $Q$, indicate that the Coulomb forces arising from the charge accumulation, require an accurate treatment. This is especially important for low-lying resonant states because they play crucial role in the analysis of the transport and optical properties of semiconductor nanostructures. Such treatment could be based on the modified transfer matrix method proposed in this paper.

In the example considered here, the shape of the Coulombic tails corresponds to a point like charge placed at $z=0$. Any other charge distribution can be treated in a similar manner. Indeed, if we look at a nanostructure from afar (from a distance much greater than its own size), details of the distribution are not discernible and it generates the same Coulombic tails as the pointlike one. Therefore, the potential tails arising from the charge accumulation, in general consist of the simple Coulombic parts (32) which in the proposed method are taken into account analytically via the Coulomb functions (40), and some non-Coulombic tails (diminishing more fast) which can be treated using the complex rotation. An example of a potential with non-Coulombic tails that require complex rotation of the coordinate is given next.

TABLE II. Coulomb modified resonance spectrum for an electron moving in the biased AlInAs/GaInAs nanostructure. The corresponding potential is shown in Fig. 8.

| $E$ (meV) | $\tau$ (ps) | $\Gamma_L$ (meV) | $\Gamma_R$ (meV) |
|---|---|---|---|
| 264.614 298 363 1 | 7953.569 05 | 0 | 0.000 082 756 8 |
| 297.154 055 222 5 | 2.670 024 248 3 | 0 | 0.246 519 184 4 |
| 623.342 644 156 4 | 0.033 580 509 9 | 6.628 723 936 2 | 12.972 294 713 0 |
| 752.698 224 505 8 | 0.018 899 501 0 | 0.042 579 506 6 | 34.784 382 291 1 |
| 874.303 431 657 1 | 0.003 881 239 8 | 1.001 575 867 9 | 168.586 574 588 5 |
| 977.294 970 954 4 | 0.003 575 776 4 | 4.980 729 346 2 | 179.094 594 044 2 |
| 1120.780 848 536 7 | 0.002 357 343 4 | 3.011 231 123 9 | 276.206 553 615 2 |

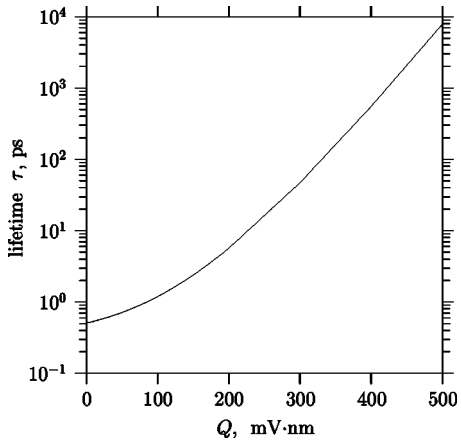


FIG. 9. Lifetime of the lowest resonance in the biased AlInAs/GaInAs nanostructure of Ref.12 as a function of the strength parameter $Q=Q_R=-Q_L$ of the Coulombic tails (32) that are added on both sides of the structure.

### C. Eckart potential

Proposed long ago,[13] when almost everything was solved analytically, the Eckart potential

$$V(z) = A_1 \frac{e^z}{1+e^z} + A_2 \frac{e^z}{(1+e^z)^2} \tag{49}$$

allows an exact solution of the Schrödinger equation in terms of hypergeometric functions. The corresponding spectrum of resonances can also be found analytically (see, for example, Ref. 14).

For $A_1=10$ and $A_2=50$ (in arbitrary units such that $\hbar^2/2\mu=1$) the potential (49) is shown in Fig. 10. In order to test the modified transfer matrix method, two upper resonant states of this potential were located. When doing this, the $z$ line was artificially divided by the points $z_0=-0.5, z_1=0$, and $z_2=0.5$ in four segments. Two central segments were treated as layers of a nanostructure and the "outer" intervals extending to $z_{-1}=-25$ and $z_3=25$ were turned to complex plane as is shown in Fig. 5 with $\theta=0.3\pi$. This value for the rotation angle was chosen in order to "open up" wide enough area of the unphysical sheet of the Riemann energy-surface by turning down the corresponding unitary cut (the theory is given in Ref. 5). The left and right "infinities," $z_{-1}$ and $z_3$, were moved away from the origin until the convergence was reached.

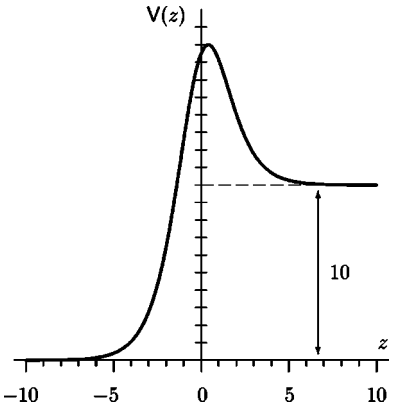


FIG. 10. The Eckart potential (49) with $A_1=10$ and $A_2=50$. The energy and distance are measured in arbitrary units such that $\hbar^2/2\mu=1$.

The energies and widths of the resonances thus found, are given in Table III together with the corresponding exact values and the results obtained in Ref. 14 by the method based on rational representation of the logarithmic derivative of the eigenfunction. As was expected, the modified transfer matrix method reproduces the exact values to a very high accuracy.

## VI. CONCLUSION

A method is developed for solving one-dimensional problems associated with semiconductor nanostructures. The method is based on the earlier proposed first-order differential equations that replace the Schrödinger equation. Using these equations, it is possible to obtain the system of fundamental solutions for each layer of a nanostructure in such form that the modified transfer matrix can be found without the rectangular discretization of the potential profile. In a sense, the traditional transfer matrix method can be considered as a particular case of the new approach, for a profile consisting of rectangular steps. Indeed, on each rectangular segment the two plane waves constitute the system of fundamental solutions of the Schrödinger equation.

The Jost and $S$ matrices can be easily constructed within the proposed method and possible bound and resonant states can be found as zeros of the Jost matrix determinant in the complex energy plane. An important feature of the new method is the possibility of calculating not only total widths of resonances but their partial widths as well. These partial

TABLE III. Two upper states of the resonance spectrum generated by the Eckart potential shown in Fig. 10. The energy is in arbitrary units such that $\hbar^2/2\mu=1$.

| $E$ | $\Gamma$ | $\Gamma_L$ | $\Gamma_R$ | Method |
|---|---|---|---|---|
| 17.870 000 000 | 3.385 616 635 | 2.027 706 9 | 1.357 909 7 | this work |
| 17.869 999 998 | 3.385 616 628 | | | Ref. 14 |
| 17.870 000 000 | 3.385 616 636 | | | exact solution |
| 17.314 164 201 | 10.188 777 872 | 7.669 590 5 | 2.519 187 3 | this work |
| 17.314 166 720 | 10.188 772 420 | | | Ref. 14 |
| 17.314 164 201 | 10.188 777 876 | | | exact solution |

widths are different for nonsymmetric potentials and determine relative probabilities of decaying of the resonances into the left and right channels as well as the probabilities of capture of the particle into a resonant state when it approaches the interaction region from the left or the right.

Within the proposed method there is a natural way of inclusion of the long-range potential tails that may arise, for example, due to the charge accumulation. The pure Coulomb tails are taken into account in an exact way, i.e., analytically.

The numerical examples given in this paper, demonstrate that the modified transfer matrix method is efficient, accurate, and takes into account long-range potential tails correctly.

In summary, there are three main features that make the proposed method unchallenged at present, namely, getting rid of the rectangular discretization, partial width calculation, and analytical treatment of the Coulomb tails.

## ACKNOWLEDGMENTS

Financial support from the University of South Africa and the National Research Foundation of South Africa (NRF Grant No. 2067421) is greatly appreciated.

## APPENDIX A: ONE-DIMENSIONAL SCATTERING REVISITED

Practically all textbooks on quantum mechanics consider one-dimensional problems as simplified examples of quantum systems. As a result, most of us have a perception that one-dimensional problems are just simple "quantum toys" having no relation to reality. This, however, is wrong. Firstly, many practical problems of modern semiconductor technology, in fact, are reduced to the one-dimensional scattering problems. And, secondly, these problems are not simple as may seem. Suffice it to say that they are inherently two-channel problems (otherwise the corresponding $S$ matrix could not be a $2\times 2$ matrix).

The two channels involved are the motion on the left and right halves of the line. The left and right channels are opened at the corresponding threshold energies $\mathsf{V}_L$ and $\mathsf{V}_R$ (see Fig. 4). Elastic scattering, i.e., pure reflection, is only possible when one of the channels is closed. The transmission is the inelastic process of the transition $L\leftrightarrow R$ between the channels.

In order to make things similar to the three-dimensional multichannel theory, let us replace the "double-infinite" axis $z\in(-\infty,+\infty)$ with the positive axis $r\in[0,+\infty)$, defined as $r=|z|$, and introduce two different potentials

$$v_L(r)=\mathsf{V}(-r)-\mathsf{V}_L \tag{A1}$$

and

$$v_R(r)=\mathsf{V}(+r)-\mathsf{V}_R, \tag{A2}$$

acting in the $L$ and $R$ channels, respectively. The introduction of $r$ can be visualized as folding of the left half of $zv$ plane around vertical axis as shown in Fig. 11. When moving from $r=\infty$ towards $r=0$, a particle moves from $z=\pm\infty$ depending on the channel which it is in, and therefore passes through

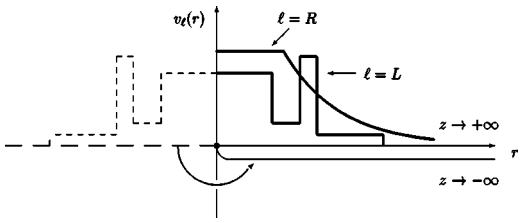


FIG. 11. Mapping of the "double-infinite" line $z\in(-\infty,+\infty)$ onto a positive line $r\in[0,+\infty)$ with the potentials $v_L(r)$ and $v_R(r)$ acting in the left and right channels.

the corresponding potential $v_\ell(r)$ with the corresponding collision energy $E-\mathsf{V}_\ell$. This is exactly what we have when deal with three-dimensional multichannel systems. For example, the dynamic variable $r$ (the distance) characterizing motion of an electron that collides with an atom, is the same no matter which state the atom was excited to, but the electron-atom interaction as well as the collision energy are different in different channels.

When the projectile particle passes the origin ($z=0$), it transits to another channel. In the picture with single variable $r$ this means that it moves backward (scattered) in another channel. If $\mathsf{V}_L\neq\mathsf{V}_R$, the particle looses or gains the amount $\Delta E=|\mathsf{V}_L-\mathsf{V}_R|$ of energy. This means that such a transition can formally be considered as an excitation (or deexcitation) of some internal degrees of freedom of the system (the target) with the excitation energy $\Delta E$. We are not interested in the physical nature of these degrees of freedom and just for the sake of formal derivations introduce the "internal Hamiltonian" $h$ associated with them and having two eigenstates

$$h|\chi_\ell\rangle=\mathsf{V}_\ell|\chi_\ell\rangle,\quad \ell=L,R, \tag{A3}$$

which are orthonormal, i.e., $\langle\chi_\ell|\chi_{\ell'}\rangle=\delta_{\ell\ell'}$. Therefore $|\chi_\ell\rangle\langle\chi_\ell|$ is the operator projecting onto the channel $\ell$, and the Hamiltonian of the whole system can be split in the three terms

$$H=H_0+v+h, \tag{A4}$$

where $H_0$ describes the free motion of the projectile with the effective mass $\mu_\ell(r)$ along the $r$ axis in the channels $L$ and $R$, i.e.,

$$\langle r|H_0|\psi\rangle=-\frac{\hbar^2}{2}\frac{d}{dr}\left[\frac{|\chi_L\rangle\langle\chi_L|}{\mu_L(r)}+\frac{|\chi_R\rangle\langle\chi_R|}{\mu_R(r)}\right]\frac{d}{dr}\psi(r), \tag{A5}$$

and the operator $v$ is the potential

$$v=v_L|\chi_L\rangle\langle\chi_L|+v_R|\chi_R\rangle\langle\chi_R|, \tag{A6}$$

with $v_L$ and $v_R$ being operators in the $r$-space, such that

$$\langle r|v_\ell|\psi\rangle=v_\ell(r)\psi(r),\quad \ell=L,R. \tag{A7}$$

As is usual in multi-channel theories, let us look for solution of the Schrödinger equation

$$H|\Psi\rangle=E|\Psi\rangle \tag{A8}$$

in the form of expansion over the target states, i.e.,

$$|\Psi\rangle = |\chi_L\rangle|\psi_L\rangle + |\chi_R\rangle|\psi_R\rangle. \tag{A9}$$

Then, multiplying Eq. (A8) from the left by $\langle r|\langle\chi_\ell|$, we obtain Schrödinger equation for wave function of the projectile in the channel $\ell$,

$$\left[-\frac{\hbar^2}{2}\frac{d}{dr}\frac{1}{\mu_\ell(r)}\frac{d}{dr} + v_\ell(r) + \mathsf{V}_\ell\right]\psi_\ell(E,r) = E\psi_\ell(E,r). \tag{A10}$$

With the definitions (A1) and (A2) of the channel potentials, it is easy to see that this equation is equivalent to the initial Schrödinger equation (1) on the line $z \in (-\infty, +\infty)$.

Combining the channel wave functions in a column

$$\psi(E,r) = \begin{pmatrix} \psi_L(E,r) \\ \psi_R(E,r) \end{pmatrix}, \tag{A11}$$

we can rewrite Eq. (A10) in the matrix form

$$\left[\frac{\hbar^2}{2}\frac{d}{dr}[\mathcal{M}(r)]^{-1}\frac{d}{dr} + \mathcal{E}\right]\psi(E,r) = \mathcal{V}(r)\psi(E,r), \tag{A12}$$

where

$$\mathcal{M}(r) = \begin{pmatrix} \mu_L(r) & 0 \\ 0 & \mu_R(r) \end{pmatrix}, \tag{A13}$$

$$\mathcal{E} = \begin{pmatrix} E - \mathsf{V}_L & 0 \\ 0 & E - \mathsf{V}_R \end{pmatrix}, \tag{A14}$$

and

$$\mathcal{V}(r) = \begin{pmatrix} v_L(r) & 0 \\ 0 & v_R(r) \end{pmatrix}. \tag{A15}$$

Matrix differential equations of the second order usually have $2N$ linearly independent column solutions if the length of the column is $N$. This is because for each element of a column, one can choose two different (that guarantee independence of the solutions) boundary conditions. Although in our case $N=2$, we can have only two independent solutions of Eq. (A12). The reason is that $\psi_L(E,r)$ and $\psi_R(E,r)$ belonging to the same column, must match at $r=0$. Indeed, on the line $z \in (-\infty, +\infty)$ they are, in fact, continuations of one another. In other words, there is one common boundary condition at $r=0$ for the upper and lower elements of each column. By the way, this same matching is the only reason why the $L$ and $R$ channels are coupled to each other since the potential (A15) is diagonal.

Combined in a square matrix,

$$\begin{pmatrix} \psi_L(E,r) \\ \psi_R(E,r) \end{pmatrix}_1 \oplus \begin{pmatrix} \psi_L(E,r) \\ \psi_R(E,r) \end{pmatrix}_2 \Rightarrow \begin{pmatrix} \psi_{L1}(E,r) & \psi_{L2}(E,r) \\ \psi_{R1}(E,r) & \psi_{R2}(E,r) \end{pmatrix} \equiv \Phi(E,r), \tag{A16}$$

these independent columns form the so-called fundamental solution matrix $\Phi(E,r)$ such that any particular solution is a linear combination of its columns.

When $r \to \infty$, all four elements of matrix (A16) behave like linear combinations of the incoming and outgoing waves in the corresponding channels. If neither of $v_\ell(r)$ has long-range Coulombic tail, all these waves $W_\ell^{(\text{in/out})}(r)$ are plane, i.e.,

$$W_\ell^{(\text{in})}(r) = e^{-ik_\ell r}, \tag{A17}$$

$$W_\ell^{(\text{out})}(r) = e^{+ik_\ell r}, \tag{A18}$$

where

$$k_\ell = \sqrt{\frac{2\mu_\ell(\infty)}{\hbar^2}(E - \mathsf{V}_\ell)}, \tag{A19}$$

is the asymptotic momentum in the channel $\ell$. If the long-range tails are present, the plane waves should be replaced with the Coulombic waves $\mathcal{G}_0(\eta,kr) \pm i\mathcal{F}_0(\eta,kr)$ constructed of the standard regular $\mathcal{F}_0$ and irregular $\mathcal{G}_0$ Coulombic wave functions, similarly to what was suggested in Ref. 15 for three-dimensional problems. In order to make further derivations general, we use the notation $W_\ell^{(\text{in/out})}$ instead of the explicit exponential functions (A17) and (A18). The asymptotic behavior of $\Phi(E,r)$ has, therefore, the following form

$$\Phi(E,r) \underset{r\to\infty}{\to} \begin{pmatrix} W_L^{(\text{in})}(r)C_{L1}^{(\text{in})} + W_L^{(\text{out})}(r)C_{L1}^{(\text{out})} & W_L^{(\text{in})}(r)C_{L2}^{(\text{in})} + W_L^{(\text{out})}(r)C_{L2}^{(\text{out})} \\ W_R^{(\text{in})}(r)C_{R1}^{(\text{in})} + W_R^{(\text{out})}(r)C_{R1}^{(\text{out})} & W_R^{(\text{in})}(r)C_{R2}^{(\text{in})} + W_R^{(\text{out})}(r)C_{R2}^{(\text{out})} \end{pmatrix}, \tag{A20}$$

where $C_{\ell n}^{(\text{in/out})}$ are some energy-dependent constants. Introducing the matrices $\mathcal{W}^{(\text{in})}(r)$ and $\mathcal{W}^{(\text{out})}(r)$ of the incoming and outgoing waves,

$$\mathcal{W}^{(\text{in/out})}(r) = \begin{pmatrix} W_L^{(\text{in/out})}(r) & 0 \\ 0 & W_R^{(\text{in/out})}(r) \end{pmatrix}, \tag{A21}$$

we can split the matrix (A20) in the following two terms

$$\Phi(E,r) \underset{r\to\infty}{\to} \mathcal{W}^{(\text{in})}(r)f^{(\text{in})}(E) + \mathcal{W}^{(\text{out})}(r)f^{(\text{out})}(E), \tag{A22}$$

where $f^{(\text{in/out})}(E)$ are the Jost matrices defined as follows

$$f^{(\mathrm{in/out})}(E)=\begin{pmatrix} C_{L1}^{(\mathrm{in/out})} & C_{L2}^{(\mathrm{in/out})} \\ C_{R1}^{(\mathrm{in/out})} & C_{R2}^{(\mathrm{in/out})} \end{pmatrix}. \tag{A23}$$

The boundary conditions defining bound state and resonance solutions should be imposed at $r\to\infty$ in such a way that there is no incoming waves. Since a physical solution $\psi^{(\mathrm{phys})}(E,r)$ is a linear combination of the columns of the fundamental solution,

$$\psi^{(\mathrm{phys})}(E,r)=\Phi(E,r)\begin{pmatrix} c_1 \\ c_2 \end{pmatrix}, \tag{A24}$$

this can be achieved by finding such combination coefficients $c_1$ and $c_2$ that the first term of the asymptotics (A22) does not contribute to the asymptotics of $\psi^{(\mathrm{phys})}(E,r)$, i.e.,

$$f^{(\mathrm{in})}(E)\begin{pmatrix} c_1 \\ c_2 \end{pmatrix}=0, \tag{A25}$$

which is possible if and only if

$$\det f^{(\mathrm{in})}(E)=0. \tag{A26}$$

A scattering state is also a linear combination of the type (A24) but with different boundary conditions at large $r$. If $A$ and $A'$ are the amplitudes of the incoming and scattered (reflected) waves in the $L$ channel, and $B$ and $B'$ the corresponding amplitudes in the channel $R$, then the scattering boundary condition reads

$$\psi^{(\mathrm{phys})}(E,r)\underset{r\to\infty}{\to}\begin{pmatrix} W_L^{(\mathrm{in})}(r)A+W_L^{(\mathrm{out})}(r)A' \\ W_R^{(\mathrm{in})}(r)B+W_R^{(\mathrm{out})}(r)B' \end{pmatrix}. \tag{A27}$$

Substituting the asymptotics (A20) of the fundamental solution into Eq. (A24) and comparing it with the boundary condition (A27), we see that

$$\begin{pmatrix} A \\ B \end{pmatrix}=f^{(\mathrm{in})}(E)\begin{pmatrix} c_1 \\ c_2 \end{pmatrix} \tag{A28}$$

and

$$\begin{pmatrix} A' \\ B' \end{pmatrix}=f^{(\mathrm{out})}(E)\begin{pmatrix} c_1 \\ c_2 \end{pmatrix}, \tag{A29}$$

which implies that the amplitudes of the incident and scattered waves are related by a $2\times 2$ matrix

$$\begin{pmatrix} A' \\ B' \end{pmatrix}=S(E)\begin{pmatrix} A \\ B \end{pmatrix}. \tag{A30}$$

This $S$ matrix

$$S(E)=f^{(\mathrm{out})}(E)[f^{(\mathrm{in})}(E)]^{-1}, \tag{A31}$$

does not depend on the choice of $A$ and $B$. We, therefore, can clarify the physical meaning of its matrix elements by considering special cases with simple choices of $A$ and $B$ as follows. If the wave is incident from the left, i.e., $A\neq 0$ and $B=0$, then $R_L=A'/A$ and $T_L=B'/A$ are the left reflection and transmission amplitudes, respectively. Similarly, if $A=0$ and $B\neq 0$ then $R_R=B'/B$ and $T_R=A'/B$ are the right reflection and transmission amplitudes. Substituting $A=0$ or $B=0$ into the equation

$$\begin{pmatrix} A' \\ B' \end{pmatrix}=\begin{pmatrix} S_{11}A+S_{12}B \\ S_{21}A+S_{22}B \end{pmatrix}, \tag{A32}$$

we see that the $S$ matrix consists of these transmission and reflection amplitudes, namely,

$$S(E)=\begin{pmatrix} R_L(E), T_R(E) \\ T_L(E), R_R(E) \end{pmatrix}. \tag{A33}$$

It should be noted, however, that in general the energy $E$ is complex and only for real energies the quantities $R_\ell$ and $T_\ell$ have the simple physical meaning. If $E$ is real, one can prove the following relations between them (see, for example, Ref. 16). When the interaction is time-reversal invariant the left and right transmission amplitudes are equal, $T_L=T_R$. Furthermore, in this case, the left and right reflection coefficients coincide as well, $|R_L|^2=|R_R|^2$, which follows from the fact that the total current is conserving, i.e., $|T_l|^2+|R_l|^2=1$.

At the energy points corresponding to bound states, and at complex energies in the resonance region (fourth quadrant) of the $E$ plane the elements of the $S$ matrix have special properties as well. Firstly, bearing in mind Eqs. (A26) and (A31), we see that at every bound state and resonance point

$$E_{\mathrm{res}}=E_r-i\frac{\Gamma}{2}, \tag{A34}$$

the $S$ matrix has a pole. Secondly, if the energy is close to $E_{\mathrm{res}}$ then

$$S_{\ell\ell'}(E)\underset{E\to E_{\mathrm{res}}}{\approx}\mathrm{const}\times\left(1-\frac{i\sqrt{\Gamma_\ell\Gamma_{\ell'}}}{E-E_{\mathrm{r}}+i\Gamma/2}\right), \tag{A35}$$

where $\Gamma_L$ and $\Gamma_R$ are the partial widths such that together they form the total width

$$\Gamma=\Gamma_L+\Gamma_R, \tag{A36}$$

of the resonance, and the ratios $\Gamma_L/\Gamma$ and $\Gamma_R/\Gamma$ are the probabilities that the resonance will decay into (or can be excited from) the $L$ and $R$ channels, respectively (see, for example, Ref. 5). From Eq. (A35) it is clear that

$$\lim_{E\to E_{\mathrm{res}}}\left|\frac{S_{LL}(E)}{S_{RR}(R)}\right|=\frac{\Gamma_L}{\Gamma_R}. \tag{A37}$$

Therefore, the partial widths can be found with the help of Eqs. (A36) and (A37), if $\Gamma$ is known and there is a procedure for the $S$-matrix calculation at complex energies.[5]

A straightforward procedure for finding the elements of the Jost matrices (A23) and, therefore, of the $S$ matrix is proposed in Sec. III. The idea is based on the special form (8) which we use to find two independent solutions of the Schrödinger equation. Indeed, comparing Eqs. (8) and (A22), we see that it must be certain relation between $C_{(L/R),j}^{(\mathrm{in/out})}$ and $F_{nj}^{(\pm)}(E,z)$ which become constants at large $r=|z|$. As is shown in Sec. III, we can choose

$$C_{Rj}^{(\mathrm{in/out})}=F_{N+1,j}^{(-/+)}(E,+\infty), \tag{A38}$$

and obtain $C_{Lj}^{(\mathrm{in/out})}$ from $F_{0j}^{(+/-)}(E,-\infty)$ with the help of the modified transfer matrix.

*Email: rakitsa@science.unisa.ac.za

[1] *Low-dimensional Semiconductor Structures*, edited by K. Barnham and D. Vvedensky (Cambridge University Press, Cambridge, 2001).
[2] E. Anemogiannis, E. N. Glytsis, and T. K. Gaylord, Microelectron. J. **30**, 935 (1999).
[3] E. J. Austin and M. Jaros, Phys. Rev. B **31**, R5569 (1985).
[4] J.-G. S. Demers and R. Maciejko, J. Appl. Phys. **90**, 6120 (2003).
[5] S. A. Rakityansky, Phys. Rev. B **68**, 195320 (2003).
[6] B. Jonsson and S. T. Eng, IEEE J. Quantum Electron. **26**, 2025 (1990).
[7] N. L. Chuprikov, Sov. Phys. Semicond. **26**, 1147 (1992).
[8] N. Imam, E. N. Glytsis, and T. K. Gaylord, Superlattices Microstruct. **29**, 411 (2001).
[9] L. Brand, *Differential and Difference Equations* (Wiley, New York, 1966).
[10] J. R. Taylor, *Scattering Theory* (Wiley, New York, 1972).
[11] *Handbook of Mathematical Functions*, edited by M. Abramowitz and A. Stegun (NBS, Washington DC, 1964).
[12] E. Anemogiannis, E. N. Glytsis, and T. K. Gaylord, Superlattices Microstruct. **22**, 481 (1997).
[13] C. Eckart, Phys. Rev. **35**, 1303 (1930).
[14] F. M. Fernández, Chem. Phys. Lett. **281**, 337 (1997).
[15] S. A. Sofianos and S. A. Rakityansky, J. Phys. A **30**, 3725 (1997).
[16] E. Merzbacher, *Quantum Mechanics* (Wiley, New York, 1998).